

PROPOSED CAVITY FOR REDUCED SLIP-STACKING LOSS

J. Eldred, Department of Physics, Indiana University, Bloomington, IN 47405, USA

R. Zwaska, FNAL, Batavia, IL 60510, USA

Abstract

This paper employs a novel dynamical mechanism to improve the performance of slip-stacking. Slip-stacking in an accumulation technique used at Fermilab since 2004 which nearly double the proton intensity. During slip-stacking, the Recycler or the Main Injector stores two particles beams that spatially overlap but have different momenta. The two particle beams are longitudinally focused by two 53 MHz 100 kV RF cavities with a small frequency difference between them. We propose an additional 106 MHz 20 kV RF cavity, with a frequency at the double the average of the upper and lower main RF frequencies. In simulation, we find the proposed RF cavity significantly enhances the stable bucket area and reduces slip-stacking losses under reasonable injection scenarios. We quantify and map the stability of the parameter space for any accelerator implementing slip-stacking with the addition of a harmonic RF cavity.

INTRODUCTION

Slip-stacking is integral to high-intensity operation at Fermilab and will likely play a central role in upgrades to the accelerator complex [1–3]. Particle loss in the slip-stacking process is a limiting factor on ultimate performance [1, 4]. Single-particle dynamics associated with slip-stacking contribute directly to the particle losses. Our previous work [5] has introduced new tools for characterizing the stable phase-space boundary of slip-stacking and evaluating particle loss in slip-stacking scenarios. A recommendation provided in this work, an upgrade of the Booster cycle-rate from 15-Hz to 20-Hz, has subsequently been incorporated into the Proton Improvement Plan (PIP-II) [1, 6]. In this paper, we propose the addition of a new 106 MHz 20 kV RF cavity to further reduce particle losses from the single-particle longitudinal dynamics of slip-stacking.

BACKGROUND

Slip-stacking is a particle accelerator configuration that permits two high-energy particle beams of different momenta to use the same transverse space in a cyclic accelerator (see [7] and [4]). The potential beam intensity of a synchrotron is doubled through the application of this technique. The two beams are longitudinally focused by two RF cavities with a small frequency difference between them. Each beam is synchronized to one RF cavity and perturbed by the other RF cavity. The proposed harmonic RF cavity has a frequency equal to twice the average of the upper and lower frequency.

This paper follows the research program outlined in [5]. Prior work in the single-particle dynamics of slip-stacking can be found in [8–10]. Fermilab has implemented slip-

stacking operationally since 2004 [4, 10, 11] and is currently applied to neutrino production for Neutrinos at Main Injector (NuMI) experiments [12–14].

Beam-loading effects can impact the effectiveness of slip-stacking. A summary of beam-loading research can be found in [5] and draws upon work on beam-loading conducted for the slip-stacking in the Fermilab Main Injector [15–18].

STABILITY WITH HARMONIC RF

The equations of motion for a single particle under the influence of two main RF cavities with frequencies separated by Δf and a harmonic RF cavity at twice the average frequency is given by:

$$\begin{aligned}\dot{\phi} &= 2\pi f_{rev} h \eta \delta \\ \dot{\delta} &= f_{rev} V_{\delta} [\sin(\phi) + \sin(\phi - \Delta f t) + \lambda \sin(2\phi - \Delta f t)].\end{aligned}\quad (1)$$

where V_{δ} is the maximum change in δ during a single revolution under the action of a single cavity [19] and λ is the ratio of the harmonic RF voltage to the main RF voltage.

Broadly speaking, slip-stacking is complicated by the fact that the two RF systems will interfere and reduce the stable bucket area. To quantify this, the literature [5, 8–10] has identified the importance of the slip-stacking parameter

$$\alpha_s = \frac{\Delta f}{f_s} \quad (2)$$

as the criterion for effective slip-stacking. Here f_s is the single-RF synchrotron frequency (see [20]). The further the buckets are away from each other in phase-space, the higher α_s is and the less interference there is. Our numerical simulation results show that a negative value of λ (bunch-lengthening mode) can counteract the interference effect that arises as the α_s decreases.

We create a stability map [5] for each value of the slip-stacking parameter α_s and the harmonic voltage ratio λ . We map the stability of initial particle positions by integrating the equations of motion for each initial position. Each position is mapped independently and only the single particle dynamics are considered. A particle is considered lost if its phase with respect to each of the first RF cavity, the second RF cavity, and the average of the two RF cavities, is larger than a certain cut-off (we used $3\pi/2$). Figure 1 shows an example of a stability without a harmonic RF cavity and with a harmonic RF cavity.

The bucket area is computed as the product of the total number of ultimately surviving points and the cell area. The slip-stacking area factor $F(\alpha_s, \lambda)$ is defined to be the ratio between the slip-stacking bucket area to that of a single-

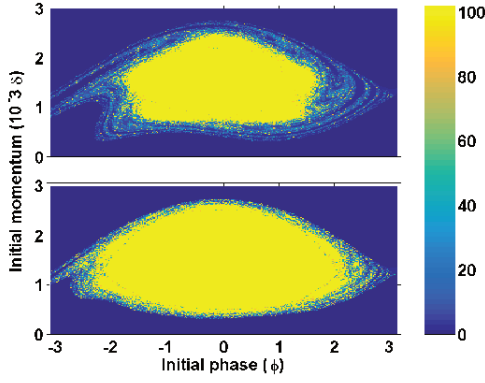


Figure 1: Stability of initial coordinates for $\alpha_s = 4.18$. The color shows the number of synchrotron periods a test particle survives before it is lost. The top plot shows a test particle survives in the status quo. The bottom plot shows slip-stacking enhanced by a harmonic RF cavity.

RF bucket with the same RF voltage and frequency:

$$\mathcal{A}_s = \mathcal{A}_0 F(\alpha_s, \lambda) = \frac{16}{h|\eta|} \frac{f_s}{f_{rev}} F(\alpha_s, \lambda). \quad (3)$$

The slip-stacking area factor $F(\alpha_s, \lambda)$ provides a method for calculating the slip-stacking stable phase-space area without requiring each case to be simulated individually [5]. Figure 2 shows the slip-stacking area factor F as a function of α_s and λ , with each datapoint calculated from its own stability map.

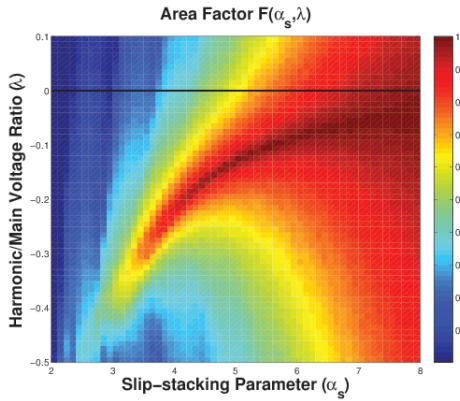


Figure 2: The slip-stacking area factor F as a function of α_s and λ .

In application, slip-stacking is tuned by varying f_s through the main RF voltage while leaving Δf unchanged. We absorb the dependence on f_s in Eq. 3 by defining the modified slip-stacking area factor $Z(\alpha_s, \lambda) = F(\alpha_s, \lambda)/\alpha_s$. This modified slip-stacking area factor Z is proportional to the slip-stacking phase-space area under voltage tuning [5]. Figure 3 shows the slip-stacking area factor Z as a function of α_s and λ .

From Figure 2 and Figure 3 it is clear that for any value of α_s , there is an optimal value of λ which maximizes the phase-space area. We term this the “balanced” condition

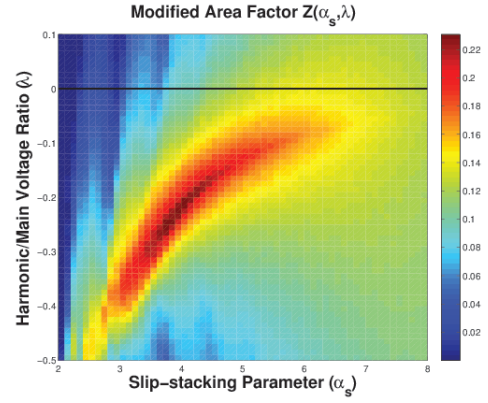


Figure 3: The modified slip-stacking area factor Z as a function of α_s and λ .

for λ . Figure 2 indicates that for $\alpha_s > 4$ at least 90% of the stable phase-space area can be recovered by using the balanced condition. Figure 3 indicates that the maximum stable phase-space area with harmonic RF is 65% higher than that without harmonic RF. $Z(\alpha_s)$ is maximized at $\alpha_s = 3.9$ for harmonic RF and is maximized at $\alpha_s = 6.2$ without harmonic RF.

Figure 4 shows that for $\alpha_s > 3$ the balanced value of λ is well-characterized as a linear function of α_s^{-2} , a term that also appears in perturbation analysis of slip-stacking [5]. The fit shown in Figure 4 is given by

$$\lambda = -3.523\alpha_s^{-2} + 0.007. \quad (4)$$

Figure 5 shows the balanced value of the harmonic RF voltage as a function of the main RF voltage. Where λ is linearly proportional to α_s^{-2} , the harmonic RF voltage is then proportional to the square of the main RF voltage. For Recycler parameters (see Table 1) and a 15-Hz Booster cycle-rate, we have $V_H = -1.773V_M^2 + 9 \times 10^{-5}$ where V_H and V_M are in units of MV. For a 20-Hz Booster cycle rate, we have $V_H = -0.997V_M^2 + 9 \times 10^{-5}$.

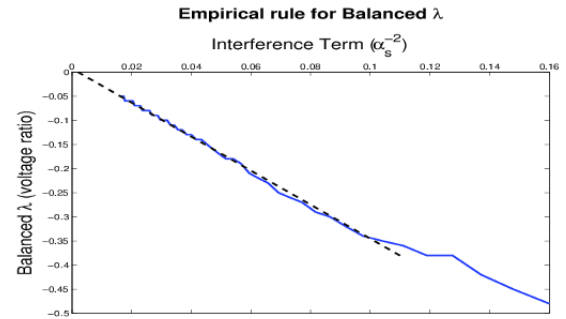


Figure 4: Balanced value of λ as a function of α_s^{-2} (blue) with a linear fit (black dashed).

When the balanced condition is reached at high α_s and low λ , the stable phase-space approaches the shape of the single-RF bucket. If the balanced condition is maintained as α_s is lowered, the stable phase-space area loses horizon-

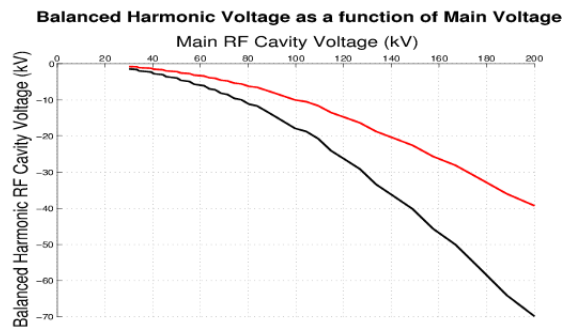


Figure 5: Balanced value of harmonic RF voltage has a quadratic dependence on main RF voltage. Bottom line shows case for a 15-Hz Booster (black) and top line for 20-Hz Booster (red).

Table 1: Recycler and Booster Parameters used in Analysis

Recycler Kinetic Energy (E)	8 GeV
Recycler Reference RF freq. (f)	52.8 MHz
Recycler Harmonic number (h)	588
Recycler Phase-slip factor (η)	-8.6×10^{-3}
Nom. Recycler RF Voltage (V)	2×100 kV
Booster harmonic number (h_B)	84
Booster cycle rate (f_B)	15/20 Hz
Difference in Recycler RF freq. (Δf)	1260/1680 Hz
Nom. Booster emittance ($\epsilon_{97\%}$)	0.12 eV·s
Nom. Booster Aspect Ratio	3.0 MeV/ns
Booster Aspect Ratio with bunch rot.	1.5 MeV/ns

tal symmetry and takes the “turtle shell” shape shown in Figure 1(b)

INJECTION SCENARIOS

The stability maps can also be used to analyze injection scenarios, by weighting the (scaled) stability maps according to a distribution that represents the number of incoming particles injected into that region of phase-space. We used this technique to identify the greatest longitudinal emittance an incoming Gaussian-distributed beam could have and still achieve 97% injection efficiency at its optimal value of α_s and λ . The 97% longitudinal beam emittance is given by $\epsilon_{97\%} = 2.17^2 \pi \sigma_p \sigma_T$

Figure 6 shows the 97% longitudinal admittance as a function of aspect ratio, with optimal choice of the main RF voltage and the harmonic RF voltage. The value of λ with the maximum injection efficiency coincides with the value of λ with the balanced condition for maximum stable phase-space area.

These results were obtained using parameter values specific to slip-stacking in the Fermilab Recycler (see Table 1) [7, 18, 21, 22], with the exception of the main RF voltage which was left unconstrained. In order to achieve the admittance shown in Figure 6 requires up to 250 kV main RF voltage and 70 kV of harmonic RF voltage. However this stable phase-space area far exceeds the requirements for

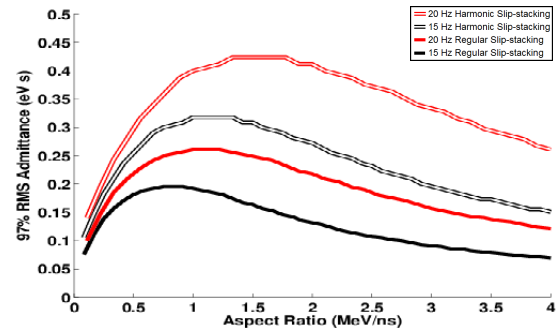


Figure 6: The 97% admittance at 97% efficiency (at an optimal α_s and λ) as a function of aspect ratio.

Table 2: Slip-stacking losses for as a function of emittance and upgrade scenario. The voltages are constrained and the aspect ratio is fixed to 1.5 MeV/ns.

Losses	Regular	Harmonic	Ratio
15-Hz with 0.10 eV·s	0.540 %	0.021 %	26.3
15-Hz with 0.12 eV·s	1.116 %	0.069 %	16.2
15-Hz with 0.18 eV·s	3.979 %	0.573 %	9.4
20-Hz with 0.10 eV·s	0.037 %	0.009 %	4.0
20-Hz with 0.12 eV·s	0.117 %	0.037 %	3.2
20-Hz with 0.18 eV·s	0.911 %	0.409 %	2.2

slip-stacking operation with minimal loss. Table 2 shows the loss-rates as a function of emittance for each of the four upgrade scenarios with main RF voltage limited to 100 kV and harmonic RF voltage limited to 20 kV.

CONCLUSION

In summary, we have introduced a harmonic RF cavity as a novel solution to enhance the stable phase-space area of slip-stacking. Our results predict the optimal RF cavity voltages and established an empirical rule relating the main RF voltage to the harmonic RF voltage. We have characterized the stable slip-stacking bucket area for any combination of accelerator parameters and have demonstrated that the harmonic RF cavity can virtually eliminate losses from longitudinal single-particle dynamics. Before installing this 106 MHz 20 kV RF cavity, however, it will be important to demonstrate that the proposed harmonic RF cavity will also reduce significantly losses in simulations which include space-charge forces and collective effects. Losses of a few percent also occur during slip-stacking from limitations on momentum aperture; A scheme for reducing the total momentum usage has been determined [5, 14], but further work should verify that the harmonic RF does not introduce any unacceptable increases in total momentum usage.

ACKNOWLEDGMENTS

This work is supported in part by grants from the US Department of Energy under contract DE-FG02-12ER41800 and the National Science Foundation NSF PHY-1205431.

REFERENCES

- [1] P. Derwent et al., Proton Improvement Plan-II December 2013, 2013, <http://projectx-docdb.fnal.gov/cgi-bin/ShowDocument?docid=1232>
- [2] C. Mariani (LBNE/DUSEL Collaborations), Proc. NOW 2010, <http://dx.doi.org/10.1016/j.nuclphysbps.2011.04.134>
- [3] J. Galambos, M. Bai, and S. Nagaitsev, Snowmass Workshop on Frontier Capability Summary Report, 2013, http://www.bnl.gov/swif2013/files/pdf/WorkshopSummary_Rev11.pdf
- [4] B. C. Brown, P. Adamson, D. Capista et al., Phys. Rev. ST Accel. Beams **16**, 071001 (2013), <http://dx.doi.org/10.1103/PhysRevSTAB.16.071001>
- [5] J. Eldred, R. Zwaska, Phys. Rev. ST Accel. Beams **17**, 094001 (2014) [<https://journals.aps.org/prstab/pdf/10.1103/PhysRevSTAB.17.094001>].
- [6] P. Derwent, S. Holmes, V. Lebedev, Fermilab Report No. BEAMS-DOC-4662-v1, 2014, https://beamdocs.fnal.gov/AD/DocDB/0046/004662/001/THIOA05_talk.pdf
- [7] J. Eldred, R. Zwaska, Proc. HB2014, <http://accelconf.web.cern.ch/AccelConf/HB2014/papers/mopab12.pdf>
- [8] F. E. Mills, Brookhaven National Laboratory Report No. 15936, 1971.
- [9] D. Boussard, Y. Mizumachi, IEEE Trans. Nucl. Sci. **26**, 3623 (1979), http://ieeexplore.ieee.org/xpls/abs_all.jsp?arnumber=4330122
- [10] J. A. MacLachlan, Fermilab Report No. FERMILAB-FN-0711, 2001, <http://lss.fnal.gov/archive/test-fn/0000/fermilab-fn-0711.pdf>
- [11] K. Seiya, T. Berenc, B. Chase et al., Proc. HB2006, www.jacow.org/abdwhb06/PAPERS/THAY02.PDF
- [12] P. Adamson et al., (MINOS Collaboration), Phys. Rev. Lett. **110**, 251801 (2013), <http://journals.aps.org/prl/abstract/10.1103/PhysRevLett.110.251801>
- [13] L. Fields et al., (MINERvA Collaboration), Phys. Rev. Lett. **111**, 022501 (2013), <http://journals.aps.org/prl/abstract/10.1103/PhysRevLett.111.022501>
- G. A. Fiorentini et al., (MINERvA Collaboration), Phys. Rev. Lett. **111**, 022502 (2013), <http://journals.aps.org/prl/abstract/10.1103/PhysRevLett.111.022502>
- [14] D. Ayres et al. (NOvA Collaboration), The NOvA Technical Design Report, FERMILAB-DESIGN-2007-01, 2007, <http://inspirehep.net/record/774999>
- [15] K. Seiya et al., Proc. PAC05, [<http://dx.doi.org/10.1109/PAC.2005.1590430>].
- [16] J. Dey, K. Koba, I. Kourbanis et al., Proc. PAC01, www.jacow.org/p01/papers/mpph048.pdf
- [17] J. Dey, I. Kourbanis, Proc. PAC05, <http://dx.doi.org/10.1109/PAC.2005.1590972>
- [18] R. Madrak, D. Wildman, Proc. PAC13, www.jacow.org/PAC2013/papers/wepma13.pdf
- [19] $V_{\delta} = \frac{eV}{\beta^2 E}$, where V is the effective voltage of the RF cavity, e is the charge of the particle, $\beta = v/c$ is the velocity fraction of the speed of light, E is the total energy of the particle. We set the voltage of each of the two main RF cavities to be equal.
- [20] S. Y. Lee, *Accelerator Physics*, 3rd Ed, ISBN: 978-9-8143-7494-1, World Scientific, Singapore, (2012).
- [21] K. Seiya, B. Chase, J. Dey et al., Proc. BEAM07, <http://cds.cern.ch/record/1133130/files/p66.pdf>
- [22] X. Yang, A. I. Drozhdin, W. Pellico, Proc. PAC07, <http://inspirehep.net/record/758224>